The Crop Journal 12 (2024) 1483–1495

Contents lists available at ScienceDirect

The Crop Journal

journal homepage: www.keaipublishing.com/en/journals/the-crop-journal/

Zinc finger protein ZFP36 and pyruvate dehydrogenase kinase PDK1 function in ABA-mediated aluminum tolerance in rice

Nana Su [a], Yanning Gong [a], Xin Hou [e], Xing Liu [b], Sergey Shabala [b,c], Vadim Demidchik [b,d], Min Yu [b], Mingyi Jiang [a], Liping Huang [a,b,*]

[a] College of Life Sciences, Nanjing Agricultural University, Nanjing 210095, Jiangsu, China
[b] International Research Center for Environmental Membrane Biology, College of Food Science and Engineering, Foshan University, Foshan 528000, Guangdong, China
[c] Tasmania Institute of Agriculture, University of Tasmania, Hobart, TAS 7001, Australia
[d] Department of Plant Cell Biology and Bioengineering, Biological Faculty, Belarusian State University, Minsk 220030, Belarus
[e] College of Life Sciences, Wuhan University, Wuhan 430072, Hubei, China

ARTICLE INFO

Article history:
Received 21 February 2024
Revised 28 April 2024
Accepted 2 June 2024
Available online 10 July 2024

Keywords:
ZFP36
OsPDK1
ABA signaling
Aluminum tolerance

ABSTRACT

Aluminum (Al) toxicity poses a significant constraint on field crop yields in acid soils. Zinc finger protein 36 (ZFP36) is well-documented for its pivotal role in enhancing tolerance to both drought and oxidative stress in rice. This study unveils a novel function of ZFP36 modulated by abscisic acid (ABA)-dependent mechanisms, specifically aimed at alleviating Al toxicity in rice. Under Al stress, the expression of *ZFP36* significantly increased through an ABA-dependent pathway. Knocking down *ZFP36* heightened Al sensitivity, while overexpressing *ZFP36* conferred increased resistance to Al stress. Additionally, our investigations revealed a physical interaction between ZFP36 and pyruvate dehydrogenase kinase 1 in rice (OsPDK1). Biochemical assays further elucidated that OsPDK1 phosphorylates ZFP36 at the amino acid site 73–161. Subsequent experiments demonstrated that ZFP36 positively regulates the expression of ascorbate peroxidases (OsAPX1) and OsALS1 by binding to specific elements in their upstream segments in rice. Through genetic and phenotypic analyses, we unveiled that OsPDK1 influences ABA-triggered antioxidant defense to alleviate Al toxicity by interacting with ZFP36. In summary, our study underscores that pyruvate dehydrogenase kinase 1 (OsPDK1) phosphorylates ZFP36 to modulate the activities of antioxidant enzymes via an ABA-dependent pathway, influencing tolerance of rice to soil Al toxicity.

1. Introduction

Aluminum (Al) toxicity impairs plant growth and yield in acidic soils [1]. Plants can alleviate aluminum toxicity through a series of strategies such as organic acid secretion and antioxidant stress enhancement. At micromolar concentrations, Al^{3+} is toxic to cells, targeting various cellular sites and impeding water and nutrient absorption [2]. A mechanism of Al tolerance is the sequestration of Al^{3+} in vacuoles, a process facilitated by tonoplast Al transporters such as the ABC transporter OsALS1 [3]. The uptake of Al is mediated by the Nramp family aluminum transporter OsNRAT1, whose expression is crucial for conferring Al tolerance [4]. Al-tolerant cultivars also exhibit a higher secretion rate of organic acids such as malate [5,6] and citrate [7] than do sensitive cultivars. These organic acids form complexes with Al (Al-OA complex), reducing its solubility [8]. Chelates of Al-OA are less toxic than free Al^{3+} [9]. In rice, the citrate-transporting MATE, OsFRDL4, participates in citrate secretion, and the amount of citrate in root exudate markedly increases under Al toxicity conditions. Al toxicity induces the accumulation of reactive oxygen species (ROS), leading to oxidative stress [10]. Scavenging ROS with antioxidants has the potential to mitigate Al toxicity [11].

ABA participates in the transduction of Al stress signals and Zinc finger proteins (ZFPs) are involved in ABA signaling [12–18]. Among the numerous transcription factor families in higher plants, the zinc finger protein family is one of the largest, containing 176 members in *Arabidopsis* and 189 members in rice, suggesting diverse functions [17,19]. A crucial subset of ZFPs is the Cys2/His2 (C2H2)-type ZFPs. This type of zinc finger features a conserved motif formed by two cysteine and two histidine residues, along with Zn^{2+}, and its core comprises an α-helix and an antiparallel double-stranded β-sheet for stabilization [18]. Rice encodes a C2H2-type transcription factor named BsrD1, which has been

* Corresponding author.
E-mail address: liphuang@fosu.edu.cn (L. Huang).

https://doi.org/10.1016/j.cj.2024.06.004

shown to increase resistance against rice blast disease [13,20]. OsZFP36 (ZFP36), directly targeting the promoters of *OsAPX1* and *Prxs*, is also involved in ABA-mediated alterations in the balance of reactive oxygen species (ROS) [13,20]. The expression and transcription of genes responsive to Al stress function in mitigating aluminum toxicity in plants [21,22]. However, it remains unclear whether and how ZFP36 is involved in alleviating aluminum toxicity. Establishing a causal link between ZFP36, ABA, and Al toxicity invites further investigation.

In plants, ABA signaling, redox-related processes and pyruvate metabolism play important roles in response to Al stress [13,23–25]. The activity of pyruvate dehydrogenase kinase (PDK), responsible for phosphorylating and negative regulating the pyruvate dehydrogenase complex (PDC), is modulated by H_2O_2 [26,27]. The PDC serves as a central metabolic machinery, influencing pyruvate levels and regulating the tricarboxylic acid cycle as well as fatty acid biosynthesis [26]. PDKs from various plant species, including *Zea mays* [28], *Oryza sativa* [29], *Arabidopsis thaliana* [30], and *Brassica napus* [31], have been identified based on sequence similarity with their mammalian counterparts. In plants, Mitochondrial pyruvate dehydrogenase participates in response to Al stress [32], and in rice, the enzyme is down-regulated by ABA and up-regulated by gibberellic acid (GA) via OsPDK1 [29]. The potential involvement of OsPDK1 in Al tolerance remains to be determined.

The objective of this study was to identify the function of ZFP36 in response to Al stress in plants, find the interaction between OsPDK1 and ZFP36, and explore the mechanism of reducing Al toxicity by influencing ABA-induced antioxidant reaction.

2. Materials and methods

2.1. Plant materials and growth conditions

The rice (*Oryza sativa* L. sub. *japonica*) cultivar Nipponbare was grown following Zhang et al. [13]. Three-day-old plants were subjected to temperatures of 28 °C (day) and 22 °C (night), with continuous 200 μmol m^{-2} s^{-1} photosynthetic active radiation, and 14 h (day)/10 h (night) photoperiod.

Tobacco (*Nicotiana benthamiana*) seeds were sown in soil substrate-filled pots under conditions of 16 h of light and 8 h of darkness at 25 °C within a growth chamber. Daily watering was applied for 20–30 d, and fresh seedlings were used for *Agrobacterium* transformation. The generation of transgenic mutants was accomplished using the transgenic system provided by Boyuan Company (Hangzhou, Zhejiang, China).

For the physiological analysis of transgenic mutants, seeds were germinated for 3 d. Then they were cultured in black 96-well plates in a 3 L plastic box at 25 °C. After 1 d, the seedlings were exposed to solutions containing 0, 10, 25, 50, and 100 μmol L^{-1} Al for 1 d at pH 4.5. Relative root elongation (RRE) under Al stress or in the control solution after 1 d was recorded to assess Al tolerance. Root lengths were measured with rulers post-treatment, and RRE was calculated as (root elongation with Al)/(root elongation without Al) × 100. The effect of pH on RRE was measured in solutions whose pH range from 4.0 to 6.5. RRE for each treatment was calculated based on monitoring at 0 and 24 h with a Root Scanner (Wseen Detection Technology Co. Ltd., Hangzhou, Zhejiang, China).

Three-day-old rice plants were subjected to 50 μmol L^{-1} $AlCl_3$ under pH 4.5 for 12 h. The shoots and roots were harvested and rapidly frozen in liquid N_2. For fluridone pretreatment, rice seeds were exposed to a nutrient solution containing 80 μmol L^{-1} fluridone (Flu) overnight. Following pretreatment, these seedlings were transferred to the nutrient solution as previously detailed [13], and served as the control group for the entire experimental period. Plants were collected and promptly frozen in liquid N_2.

2.2. RNA isolation and RT-qPCR

Real-time quantitative reverse transcriptase-PCR (RT-qPCR) was conducted to measure gene expression. The procedures for RNA extraction and RT-qPCR followed Ni et al. [25]. Total RNA was extracted using a RNAiso Plus kit (Dalian, Liaoning, China).. About 2 μg of total RNA was obtained and reverse-transcribed with an oligo $(dT)_{16}$ primer and Moloney murine leukemia virus reverse transcriptase (TaKaRa). Gene expression was detected by RT-qPCR following the MIQE guidelines with standard curve method [25]. Table S1 describes the primers used. The relative expression levels of genes were normalized to the internal control genes *Actin* or *Histone 3*, as illustrated in Fig. S6.

2.3. Subcellular localization of OsPDK1

The *35S:OsPDK1-YFP* fused construct or *35S::YFP* was introduced into *Agrobacterium* strain GV3101, which was then transformed into 28-day-old tobacco leaves. Following infection with *Agrobacterium* strain GV3101, the plants were cultivated for 1–2 d, and YFP signals in the leaves were visualized using a Zeiss LSM710 Laser Scanning Confocal Microscope[33].

2.4. ChIP-sequencing and ChIP RT-PCR

ChIP-seq is described by Hang [14]. In the ChIP RT-PCR experiment, the ZFP36-interacting DNA sequence was acquired as previously outlined [14]. Two segments of the DNA sequences from the *OsALS1* promoter (P1 and P2) were subjected to analysis by RT-PCR using the designated primers (refer to Table S1).

2.5. Y2H-gold yeast two-hybrid screening and yeast one-hybrid assay

To identify protein interactions between ZFP36 and OsPDK1, we conducted a yeast two-hybrid assay (Y2H) using the Clontech Yeast Y2H-Gold Two-Hybrid System (Clontech). The coding sequence (CDS) of *OsPDK1* was Inserted into the pGBKT7 vector at *NcoI* and *SmaI* sites to create the bait vector, which was then transformed into the *Saccharomyces cerevisiae* strain Y2H gold. The prey cDNA library derived from rice leaves was fused to pGADT7. Cultivation of cells on SD agar plates lacking Leu, Trp, His, Ade (SD/-Leu/-Trp/-His-Ade) allowed for the screening of transformed cells. Potential positive transformants were identified with an antibiotic assay using aureobasidin A (AbA^r) and α-galactosidase activity, assessed with the chromogenic substrate X-α-gal (5-bromo-4-chloro-3-indolyl α-D-galactopyranoside). Plasmids pGADT7 encoding candidate OsPDK1-interacting proteins were detected and isolated with Genewiz company (Genewiz Biotech, Co., Ltd, Suzhou, Jiangsu, China).

A yeast one-hybrid test was conducted using AH109. The putative ZFP36 binding sites on the *OsALS1* promoter, identified as P1 ((−1400 bp) to (−900 bp)) and P2 ((−400 bp) to (+1 bp)) through ChIP-seq, were selected for the assay. These two segments (P1, P2) were incorporated into the *pAbAi* vector to generate the bait constructs. The coding sequence of ZFP36 was fused to pGADT7 to produce the prey construct. Co-transformation of the bait and prey constructs was carried out in the yeast strain AH109, and the transformed yeasts were transferred to a selective medium (SD/-Leu). The identification of positive clones was confirmed by their growth on SD/-Leu medium supplemented with the specified concentration of AbA^r.

2.6. Protein prokaryotic heterologous expression

ZFP36 was fused with GST in the pGEX-4 T-1 vector to generate the GST-ZFP36 construct. To induce the expression of GST-ZFP36 proteins, bacterial solutions, of *E. coli* strain BL21 (DE3) carrying these vectors along with empty vectors, were subjected to treatment with 0.5 mmol L^{-1} isopropyl 1-thio-β-D-galactopyranoside (IPTG) in Luria-Bertani broth for 5–6 h at 25 °C. *OsPDK1* was cloned into the pET-30a (Novagen) vector with a His tag to construct OsPDK1-His. These recombinant proteins were transformed into *E. coli* strain BL21 (DE3) to facilitate the expression of the target proteins. Cultivation was at 22 °C with 0.1 mmol L^{-1} IPTG for 6 h on a shaker at 160 r min^{-1} to induce protein production.

2.7. GST pulldown assay

To study the interaction between ZFP36 and OsPDK1 *in vitro*, a GST pulldown assay was performed following Zhu et al. [33]. OsPDK1 fused with His-tag was purified with High Affinity Ni-NTA Magnetic beads (Genescript, USA). GST and GST-ZFP36 were tethered on glutathione-Sepharose-4B Magnetic beads, and the purified His-OsPDK1 was added into the Magnetic beads bound with GST or GST- ZFP36. The reaction solutions were purified with binding buffer (140 mmol L^{-1} NaCl, 10 mmol L^{-1} KCl, 4.2 mmol L^{-1} Na_2HPO_4, 2 mmol L^{-1} KH_2PO_4, 10% BSA, pH 7.2) and incubated at 4 °C for at least 2 h. The beads were then washed with wash buffer (400 mmol L^{-1} NaCl, 10 mmol L^{-1} KCl, 4.2 mmol L^{-1} Na_2HPO_4, 2 mmol L^{-1} KH_2PO_4, pH 7.2) at least five times. The samples were separated by 12% SDS-PAGE and were detected by Western blotting using mouse anti-His antibody (Sigma-Aldrich, USA), and goat-anti-mouse horse radish peroxidase (HRP)-conjugated secondary antibody (Sigma-Aldrich, USA).

2.8. BiFC assays

To study the interaction between ZFP36 and OsPDK1 *in vivo*, we conducted Bimolecular Fluorescence Complementation (BiFC) using split Yellow Fluorescent Protein (YFP) and Firefly Luciferase (LUC). For YFP recombination, the coding region of *ZFP36* was cloned into the pSPYCE vector, generating the YFP^C-*ZFP36* construct [14,15]. *OsPDK1* was cloned into the *KpnI* and *SmaI* sites of the pSPYNE vector to produce the YFP^N-*OsPDK1* construct. Onion (*Allium cepa*) epidermal layers were placed on Murashige and Skoog (MS) solid medium, and the two YFP^N/YFP^C or fusion proteins were transiently introduced into onion cells by gene-gun bombardment (Biolistic PDS-1000/He Particle Delivery System; Bio-Rad) as previously detailed [33].

For LUC recombination, the coding sequence of *ZFP36* was fused to the C or N terminal of LUC, while the *OsPDK1* coding region was also cloned to the C-terminal or N-terminal of LUC to generate *cLUC-ZFP36*, *nLUC-OsPDK1*, *nLUC-ZFP36*, and *cLUC-OsPDK1* fusion proteins. For negative control, the coding sequence of 1–73 amino acid of *ZFP36* sequence was fused to the C or N terminal to generate the *cLUC-ZFP36*^{T2} and *nLUC-ZFP36*^{T2} fusion protein. These constructs were then introduced into 28-day-old *N. benthamiana* leaves using *Agrobacterium tumefaciens* strain EHA105. After incubation for 2–3 d, leaf protein homogenate was subjected to the LUC activity assay.

2.9. Antioxidant enzyme assay

Rice seedlings (0.5 g) were ground to powder in liquid nitrogen. The samples were dissolved in 3 mL of potassium phosphate buffer (1 mmol L^{-1} EDTA, 1% polyvinylpyrrolidone (PVP), 50 mmol L^{-1}, pH 7.0) in the dark. The solution was centrifuged at 12,000×*g* at 4 °C for 30 min. Total protein content was quantified by the Bradford method with a standard curve made with BSA protein (Wuhan, Hubei, China) at 595 nm, and antioxidant enzyme activity as superoxide dismutase (SOD), ascorbate peroxidase (APX), catalase (CAT) was measured as described previously [23].

2.10. GUS activity

The Quantitative GUS Activity Assay of Plant Extracts kit from Beyotime Biotechnology (Beijing, China) was used for measuring 4-MU content. 4-MU was quantified by exciting at 365 nm and measuring emission at 455 nm.

2.11. Immunoprecipitation kinase activity assay

Kinase activity assay was performed in the immunocomplex incubated with 2 μg substrates (maltose binding protein (MBP) or recombinant His-ZFP36) in the reaction buffer [25 mmol L^{-1} Tris, pH 7.8, 1 mmol L^{-1} dithiothreitol (DTT), 2.5 mmol L^{-1} $CaCl_2$, 5 mmol L^{-1} $MgCl_2$ with 200 nmol L^{-1} ATP plus 1 μCi of $[\gamma-^{32P}]$ATP (3000 Ci mmol L^{-1}) containing 10 μg GST-ZFP36 and OsPDK1-His for 30 min following Ma et al. [34]. For measuring OsPDK1 kinase activity, OsPDK1 was immunoprecipitated using anti-OsPDK1 (C-terminus of OsPDK1 was used to generate OsPDK1 antibody) from variously treated rice roots, and the activity was detected through the substrate MBP.

3. Results

3.1. Physiological analysis of ZFP36 transgenic plants in Al tolerance

In the absence of Al, the root elongation of mutant plants was indistinguishable from that of wild-type (WT) plants (Figs. 1A, S1C, D). However, under different Al concentrations, it was lower (Figs. 1A, S1C, D). The relative root elongation (RRE) inhibition in *ZFP36*-RNAi was 27.1%, 64.4%, and 84.7%, respectively, under 25, 50, and 100 μmol L^{-1} Al treatment at pH 4.5 (Fig. 1B). In comparison, these values for WT plants were 23.3%, 53.6%, and 68%, respectively (Fig. 1B). Overexpression of *ZFP36* increased Al tolerance, with RRE inhibition being 18.1%, 32.3%, and 46.5%, respectively, when treated with 25, 50, and 100 μmol L^{-1} Al, compared to WT plants (Fig. 1B). No differences in root growth were observed in response to variations in medium pH (tested for *ZFP36*-OE, WT, and *ZFP36*-RNAi; Fig. 1C).

3.2. ZFP36 expression pattern and its ABA regulation under Al treatment

ZFP36 was more highly transcribed in both roots and shoots under Al treatment, and higher in roots (Fig. 1D). The GUS activity results aligned with the RT-qPCR findings, as transgenic *pZFP36:GUS* plants displayed higher 4-methylumbelliferyl β-D-glucuronide (MUG) content in roots than in shoots (Fig. S2). Under control conditions, the transcript level of *ZFP36* in basal roots (10–20 mm) exceeded that in the root apex (0–5 mm) (Fig. 1E). Al treatments stimulated the expression of *ZFP36* in roots, particularly in the intermediate zone (5–10 mm) between the apical zone and elongation zone (Fig. 1E). *ZFP36* expression was induced by ABA (Fig. 1G). Fluridone (Flu), an inhibitor of ABA biosynthesis, led to a reduction in Al-induced *ZFP36* expression (Fig. 1G).

3.3. OsPDK1 physically interacts with ZFP36 in vivo and in vitro

ZFP36 may regulate diverse physiological processes by associating with other proteins. To explore the underlying molecular mechanism by *ZFP36* participate in ABA-mediated detoxification

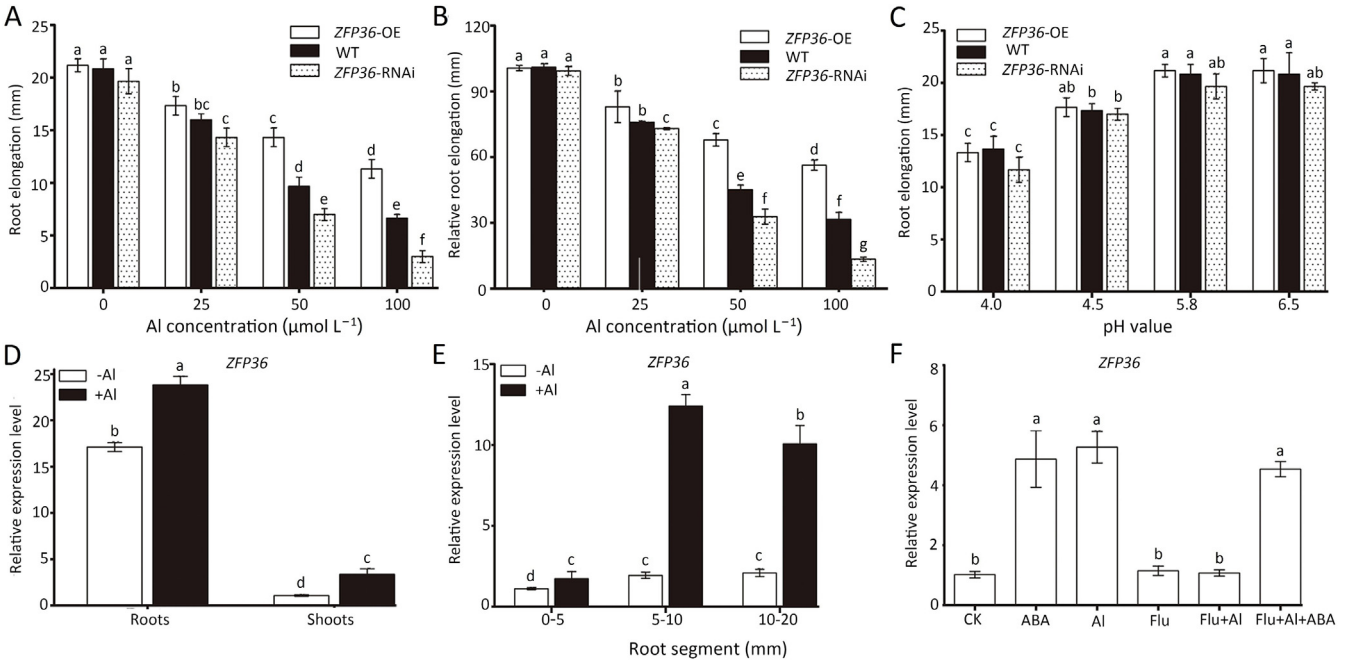

Fig. 1. The elongation analysis of roots in *ZFP36*-OE, *ZFP36*-RNAi rice plants under Al toxicity, and the expression pattern of *ZFP36*. (A,B) The influence of Al on the root elongation (A) and relative root elongation (B) of wild-type (WT) rice, *ZFP36* overexpressing plants (*ZFP36*-OE), and RNA-induced ZFP36 silencing plants (*ZFP36*-RNAi). Root length was measured at different treatment. (C) Response of ZFP36-OE, ZFP36-RNAi plants to solution with different pHs. Seedlings of three-day-old WT plants and *ZFP36*-OE, *ZFP36*-RNAi plants were treated with solutions with various pH for 24 h. The length of the root was obtained at 0 h and 24 h. (D) The expression of *Histone3* in rice plants treated with a solution containing 0, 25, 50 or 100 μmol L^{-1} $AlCl_3$ for 24 h at pH 4.5, *Actin1* was used as the internal control. (E–G) The expression patterns of *ZFP36* in roots or shoots. Three-day-old rice plants at pH 4.5 were treated with or without 50 μmol L^{-1} $AlCl_3$ for 6 h, the shoots and roots were collected. (E) The root segments (0–5, 5–10 and 10–20 mm) were treatment with 50 μmol L^{-1} AlCl3 at pH 4.5 for 6 h and cut with a razor. (F) Rice seeds were treated with or without fluridone (Flu), an ABA inhibitor, for 8 h, and with 50 μmol L^{-1} ABA for 30 min after exposure to 50 μmol L^{-1} $AlCl_3$ for 12 h and the roots were collected (G). *ZFP36* level was detected using RT-qPCR, and *Histone 3* was used as an internal control. Values are means ± SD (n = 50 for A-C, n = 3 for E–G). Means labeled with the same lowercase letter did not differ at $P < 0.05$.

of aluminum in rice, we performed yeast 2-hybrid (Y2H) screening from a pool of key regulatory proteins that act in the response to Al. The results presented in Fig. 2A demonstrate a direct interaction between ZFP36 and OsPDK1 in yeast (Fig. 2A). The entire OsPDK1 coding sequence was cloned using primers (Table S1) designed based on the rice database (https://rapdb.dna.affrc.go.jp/). CDS spans 1092 base pairs, with an identical sequence to the database, encoding a protein of 363 amino acids (aa) (Fig. S3).

To corroborate the findings of the Y2H test, we performed both *in vitro* and *in vivo* assays to validate the ZFP36-OsPDK1 interaction. For *in vivo* experiments, BiFC assays to test YFP signals, luciferase (LUC) imaging experiments, and co-immunoprecipitation (CoIP) assays were conducted. In the BiFC assay to test YFP signals, ZFP36 was fused to YFP^C, and OsPDK1 was fused to YFP^N (Fig. 2B). However, co-expressing YFP^N-OsPDK1 and ZFP36-YFP^C in onion epidermal cells did not yield observable YFP fluorescence in combinations involving YFP^C and YFP^N-OsPDK1 or ZFP36-YFP^C and YFP^N (Fig. 2B). A robust fluorescence signal was observed exclusively in the nucleus, suggesting that the OsPDK1-ZFP36 complex was localized in the nucleus. To assess LUC imaging in the BiFC assay, ZFP36 was fused to the C-terminal of luciferase (LUC^C), and OsPDK1 was fused to the N-terminal LUC fragment (LUC^N). Co-expression of OsPDK1-LUCN and LUC^C-ZFP36 in tobacco cells resulted in detectable LUC imaging, while combinations involving OsPDK1-LUC^N with LUC^C-$ZFP36^{T2}$ or LUC^C-OsPDK1 with $ZFP36^{T2}$-LUC^N did not exhibit the LUC signal (Fig. 2C). In the CoIP assay, OsPDK1 with a Flag tag (OsPDK1-Flag) and ZFP36 with a Myc tag (Myc-ZFP36) were transiently co-expressed using a PEG-mediated transformation approach in rice protoplasts. The results in Fig. 2E show detection of Myc-ZFP36 with anti-Myc when OsPDK1-Flag and Myc-ZFP36 were co-expressed in protoplasts (Fig. 2E, left column). In contrast, overexpressing OsPDK1-Flag (Fig. 2E, middle column) or Myc-ZFP36 alone (Fig. 2E, right column) did not yield the Myc band. This confirms the *in vivo* interaction between OsPDK1 and ZFP36.

To assess the interaction between ZFP36 and OsPDK1 *in vitro*, we expressed OsPDK1 with a His tag (OsPDK1-His) and ZFP36 with glutathione S-transferase (GST-ZFP36) in *E. coli* to perform an *in vitro* GST pull-down assay. The GST-ZFP36 protein incubated with OsPDK1-His successfully pulled down the His-OsPDK1 protein (Fig. 2D, left column). In contrast, neither GST-ZFP36 nor GST alone pulled down the His-OsPDK1 protein (Fig. 2D, right column). This result establishes that OsPDK1 interacts with ZFP36 *in vitro*.

To verify whether OsPDK1 can phosphorylate ZFP36, an "immunocomplex kinase activity assay" was employed to determine if purified His-ZFP36 could serve as a substrate (Fig. 2F, right panel). As depicted in Fig. 2F, a phosphorylation band was observed, indicating that ZFP36 is indeed a phosphorylation substrate for OsPDK1 *in vitro*. In summary, these findings suggest that the kinase protein OsPDK1 can both interact with and phosphorylate the zinc finger protein ZFP36.

To further identify the phosphorylation site of ZFP36 by OsPDK1, we analyzed potential phosphorylation sites using KinasePhos_2.0. His-tagged truncations of ZFP36, encompassing amino acids 1–220 (T0), 1–162 (T1), 1–73 (T2), 1–73 plus 162–220 (T3), 162–220 (T4), and 73–162 (T5), were generated. Y2H tests and GST pull-down assays demonstrated that only His-tagged truncations of ZFP36 containing amino acids 73–162 (T0, T1, and T5) could interact with OsPDK1 (Fig. S4A and B). Iin the *in vitro* kinase assay, OsPDK1 phosphorylated the site encompassing amino acids 73–162 of ZFP36 (Fig. S4C).

3.4. Subcellular localization of OsPDK1

Structural analyses have revealed that OsPDK1 possesses features characteristic of proteins involved in heavy metal metabolism. It

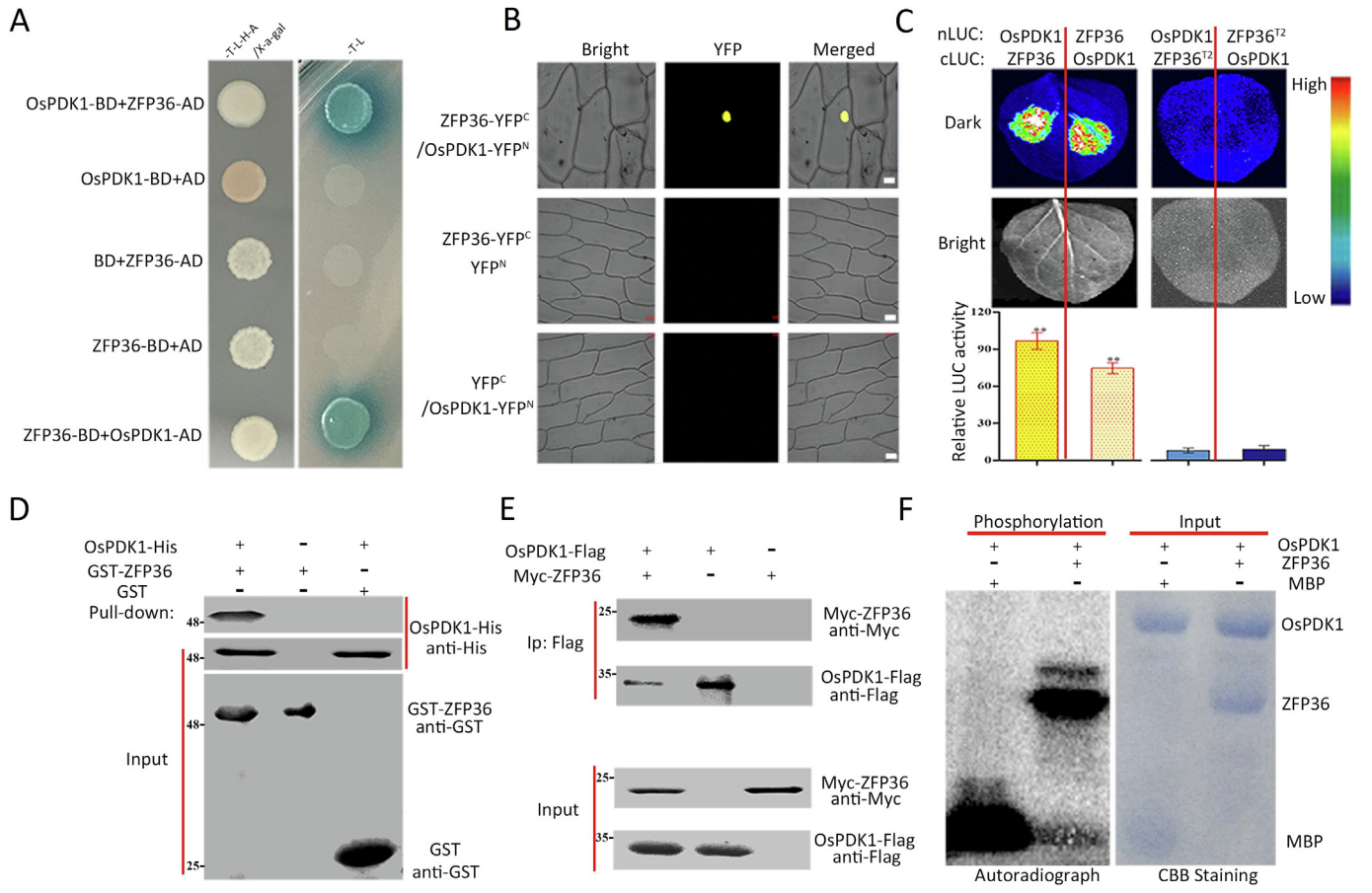

Fig. 2. The direct interaction of ZFP36 and OsPDK1 *in vitro* and *in vivo*. (A) Y2H Gold yeast assay. On control medium [SD/-Leu/Trp (SD/-L-T)] and selective medium [SD-Leu/Trp/-His/-Ade plus X-a-gal (SD-L-T-H-A/X-a-gal/)], yeast transformers with reconstructed BD and AD were plated. SD, synthetic dropout. (B) Interaction of ZFP36 and OsPDK1 in onion (*Allium cepa*) epidermal cells. YFP signals were detected by laser confocal scanning microscope. Scale bars, 50 μm. (C) Luciferase (LUC) complementation imaging assay. The upper panel shows images and luminescence of *Nicotiana benthamiana* leaves containing the indicated combinations of nLUC- and cLUC- fusions and cLUC-ZFP36^{T2} + nLUC-OsPDK1 or cLUC-OsPDK1 + nLUC-ZFP36^{T2} were used as the negative control. The lower panel is the quantification results of LUC activity in these leaves. (D) GST pull-down assay. GST-ZFP36 or GST alone were purified independently (left figure), and OsPDK1-His was detected by Western blotting. (E) CoIP test. Myc-ZPF36 and OsPDK1-flag were coexpressed in rice protoplast, and Myc-antibody was used to immunoprecipitate the protein complex, then the Flag-antibody was used to WB test. (F) *In vitro* phosphorylation of OsPDK1 to ZFP36. OsPDK1-His and GST-ZFP36 were obtained by *Escherichia coli*. Maltose binding protein (MBP) or GST-ZFP36 served as the substrate in the in-gel kinase experiment. The experiments were repeated at least three times with similar results.

includes the mitochondrial branched-chain alpha-ketoacid dehydrogenase kinase domain (BCDHK_Adom3, spanning from 24 aa to 186 aa) (Fig. S3, underscored in black) and the heavy metal sensor kinase domain (cztS_silS_copS from 262 aa to 343 aa) (Fig. S3, underscored in green), implying a potential role in sensing toxic metals. OsPDK1 exhibits three distinct spliceosomes (https://rapdb.dna.affrc.go.jp/), suggesting versatility in its functions. High sequence similarity with all PDKs is observed, with identity percentages of 91%, 63%, 73%, and 75% with ZmPDK2, ZmPDK1, AtPDK, and MtPDK, respectively (Fig. S3A). The conserved histone kinase domain is evident among PDK proteins (Fig. S3B, enclosed in a blue box).

Given that PDKs inhibit the pyruvate dehydrogenase complex in the mitochondrion [29], we sought to identify the subcellular location of OsPDK1. Through *A. tumefaciens* EHA105-mediated infiltration, we transiently introduced a fused protein (OsPDK1-GFP) into the epidermal cells of tobacco. In cells expressing the control GFP, the signal was observed in both the nucleus and cytoplasm (Fig. S5). In contrast, cells expressing OsPDK1-GFP exhibited a widespread GFP signal, particularly in the nucleus and cytosol (Fig. S5). Thus, the nucleus and cytoplasm are the primary sites for OsPDK1 expression *in vivo*.

3.5. Al effects on OsPDK1 via ABA

We monitored the expression (Fig. 3A, B), protein content (Fig. 3C), and kinase activity (Fig. 3D) of OsPDK1 when exposed to 50 μmol L^{-1} ABA or 50 μmol L^{-1} $AlCl_3$ at pH 4.5. As depicted in Fig. 3A–D, the expression, protein content, and kinase activity of OsPDK1 in rice roots were measured under ABA or Al treatment. For both ABA and Al treatments, *OsPDK1* expression initially experienced inhibition, reaching a nadir within the first 45 min (for ABA treatment) or 12 h (for Al treatment). Similarly, the accumulation of OsPDK1 protein was suppressed by ABA or Al initially, with the lowest point occurring within 30–60 min (for ABA treatment) or 12 h (for Al treatment) (Fig. 3A–D, the lower panel of 3C, 3D for ABA treatment, the upper panel of 3C, 3D for Al treatment). The kinase activity of OsPDK1 also showed initial inhibition by ABA or Al, with the lowest point occurring within 30–60 min (for ABA treatment) or 12 h (for Al treatment). The levels of gene expression, protein content, and kinase activity of OsPDK1 gradually returned to control levels after 120 min, 60 min, and 60 min, respectively, following ABA treatment, and after 24 h for all three levels following Al treatment. Subsequently, *OsPDK1* expression, the accumulation of OsPDK1 protein, and the kinase activity of

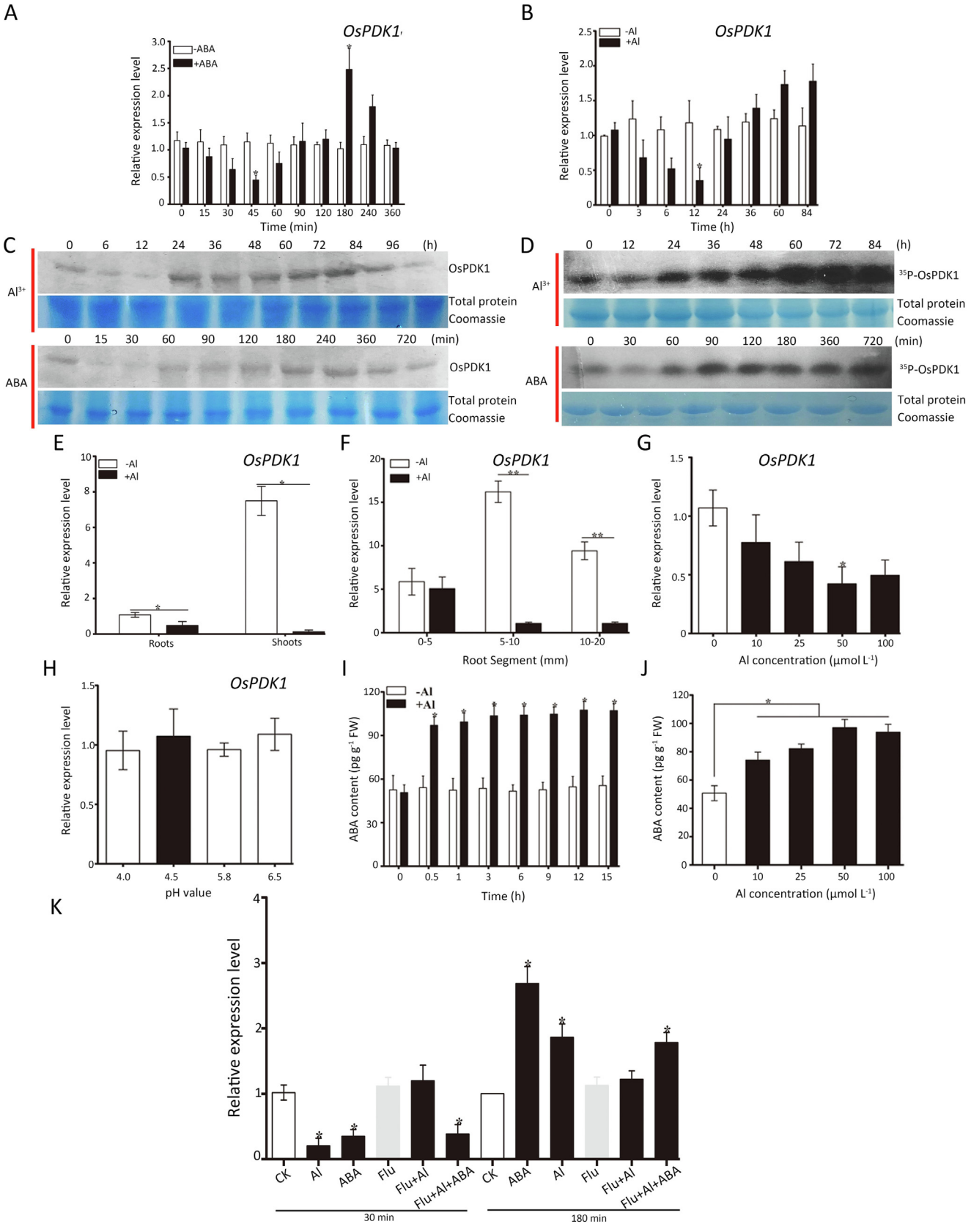
A
OsPDK1
-ABA
+ABA
Relative expression level
Time (min)
B
OsPDK1
-Al
+Al
Relative expression level
Time (h)
C
Al3+
OsPDK1
Total protein
Coomassie
ABA
OsPDK1
Total protein
Coomassie
D
Al3+
35P-OsPDK1
Total protein
Coomassie
ABA
35P-OsPDK1
Total protein
Coomassie
E
OsPDK1
-Al
+Al
Relative expression level
Roots
Shoots
F
OsPDK1
-Al
+Al
Relative expression level
Root Segment (mm)
G
OsPDK1
Relative expression level
Al concentration (μmol L-1)
H
OsPDK1
Relative expression level
pH value
I
-Al
+Al
ABA content (pg g-1 FW)
Time (h)
J
ABA content (pg g-1 FW)
Al concentration (μmol L-1)
K
Relative expression level
CK
Al
ABA
Flu
Flu+Al
Flu+Al+ABA
30 min
180 min

OsPDK1 were activated, with peaks observed at 180 min for ABA treatment and 60 h for Al treatment. This suggests that OsPDK1's kinase activity and expression may be initially inhibited by ABA and Al, followed by induction at later stages.

To investigate whether the tissue-specific expression pattern of *OsPDK1* mirrors that of *ZFP36*, we conducted RT-qPCR analysis, revealing that *OsPDK1* is expressed in both roots and shoots (Fig. 3E). The expression of OsPDK1 was more prominent in shoots than in roots in the absence of Al. However, upon exposure to Al, *OsPDK1* expression decreased, leading to higher expression in roots than in shoots (Fig. 3E). Consequently, Al treatment altered the distribution of *OsPDK1*, and the root expression pattern of *OsPDK1* (Fig. 3E) resembled that of *ZFP36* under Al stress (Fig. 1D).

Under control conditions, the transcript level of *OsPDK1* was lower in the root tip (0–5 mm) than in basal zones (10–20 mm) (Fig. 3F). *OsPDK1* expression in the root tip (0–5 mm) remained unaffected by Al treatment. However, Al-inhibited *OsPDK1* expression was observed in the basal zones (10–20 mm) and the intermediate zone between the apical and mature zone, which showed higher expression of *OsPDK1* than other zones (Fig. 3F). The inhibitory effect of Al saturated at a concentration of 50 μmol L^{-1} (Fig. 3G). The transcript level of *OsPDK1* in the roots was not influenced by high acidity (Fig. 3H), indicating that OsPDK1 is modulated specifically by Al.

To assess whether ABA contributes to the rice response to Al, we measured the endogenous ABA level in root tips exposed to varying Al concentrations at pH 4.5 (Fig. 3J). OsPDK1 accumulation occurred in response to Al concentrations ranging from 10 to 50 μmol L^{-1}, whereas the ABA content did not increase at higher Al levels (Fig. 3J). However, ABA levels increased rapidly within 0.5 h in response to 50 μmol L^{-1} $AlCl_3$ at pH 4.5 and remained relatively stable thereafter (Fig. 3I). This suggests that ABA accumulation plays a role in the plant response to aluminum. The inhibitor of ABA biosynthesis, fluridone (Flu), mitigated the inhibitory action of ABA on the expression of *OsPDK1* (Fig. 3K), indicating that the effect of Al on *OsPDK1* is mediated by ABA accumulation.

3.6. OsPDK1 is involved in ABA-induced antioxidant defense, citrate secretion and Al transporter activity to participate in Al response

To assess the role of OsPDK1 in Al stress, we generated *OsPDK1* overexpression (*OsPDK1*-OE) and *OsPDK1* knockout (*OsPDK1*-KO) plants using CRISPR-Cas9 technology. The expression levels of *OsPDK1* in *OsPDK1*-OE plants were measured, revealing a 5-fold, 14-fold, and 30-fold increase in transcript levels compared to the control in lines #1, #2, and #3 of *OsPDK1*-OE plants (Fig. S6A). The genomes of the two *OsPDK1*-KO lines had a 1-bp insertion (*OsPDK1*-KO1) and a 1-bp deletion (*OsPDK1*-KO2) in the first exon compared to the wild-type genome (Fig. S6B). Under normal conditions without Al treatment, the root lengths of *OsPDK1*-OE and *OsPDK1*-KO plants were similar to those of wild-type plants (Fig. S1A, B). However, when exposed to Al treatment, root elongation was more inhibited in *OsPDK1*-OE (#1 and #2) plants compared to wild-type plants (Fig. S1A, B). The relative root elongation (RRE) inhibition in #1 and #2 was 67.1% and 68.4%, respectively, upon 50 μmol L^{-1} Al treatment at pH 4.5 (Fig. S1B), whereas it was 50.6% in wild-type plants (Fig. S1B). In contrast, *OsPDK1* knockout (KO1 and KO2) plants exhibited increased Al tolerance, with RRE inhibition of 28.1% and 30.5%, respectively, when treated with 50 μmol L^{-1} Al at pH 4.5 (Fig. S1B). These results show that OsPDK1 is essential for Al tolerance in rice.

To unravel the mechanism underlying OsPDK1's role in Al tolerance, we examined the expression of key antioxidant genes, including *OsSODCc2* (*SODCc2*), *OsAPX1*, and *OsCatB* (*CatB*), as well as the activities of antioxidant enzymes—superoxide dismutase (SOD), ascorbate peroxidase (APX), and catalase (CAT). Our findings revealed that the overexpression of *OsPDK1* led to a notable decrease in the expression of *SODCc2*, *OsAPX1*, and *CatB* (Fig. 4A, C, E) and a reduction in the activities of SOD, CAT, and APX (Fig. 4B, D, F). In contrast, the knockout of *OsPDK1* or ABA treatment in rice elevated the expression levels of *OsAPX1*, *CatB*, and *SODCc2* (Fig. 4A, C, E) and increased the activities of APX, CAT, and SOD compared to the control group (Fig. 4B, D, F). *OsPDK1*-KO1 showed a higher response to ABA treatment (Fig. 4). These results suggest that OsPDK1 plays a role in ABA-mediated antioxidant defense against Al toxicity.

Expression of *OsALS1*, *OsFRDL4*, and *Nrat1* was induced by ABA (Fig. **S7**). In *OsPDK1*-overexpressing (*OsPDK1*-OE) rice plants, the expression of *OsALS1* and *Nrat1* was lower than in WT plants (Fig. S8A, C), while the knockout of *OsPDK1* led to an increase in the expression level of *OsALS1* and *Nrat1* compared to WT plants (Fig. S8A, C). This suggests that *OsALS1* and *Nrat1* are modulated by OsPDK1. Correspondingly, the Al content in the root apex was highest in *OsPDK1-OE* rice plants and lowest in *OsPDK1*-knockout (*OsPDK1*-KO) plants (Fig. S8E). In contrast, the expression of *OsALS1* and *Nrat1* increased in *ZFP36*-overexpressing (*ZFP36*-OE) rice plants and decreased in *ZFP36*-RNAi rice plants. *ZFP36*-RNAi rice plants accumulated the most Al, while *ZFP36*-OE rice plants accumulated the least Al in the root apex (Fig. S8B, D, F). The expression of *OsFRDL4* and citrate secretion decreased in *OsPDK1*-OE and *ZFP36*-RNAi rice plants, while it increased in *OsPDK1*-KO and *ZFP36*-OE plants, especially under Al treatment (Fig. S9). This implies that *OsFRDL4* is downregulated by OsPDK1 but upregulated by ZFP36.

3.7. OsPDK1 inhibits ZFP36 transcription activity

OsPDK1 establishes a direct interaction with ZFP36 and phosphorylates this protein, as illustrated in Fig. 2. Chip-seq analysis uncovered that ZFP36 targets numerous antioxidant defense enzymes and Al transporters. ZFP36 is a transcriptional enhancer of *OsAPX1* [14,15], and OsPDK1 is involved in the regulation of *OsAPX1*, *CatB*, and *SODCc2* (Fig. 4A, C, E), as well as APX, CAT, and SOD activities (Fig. 4B, D, F). Thus, OsPDK1 functions in the

Fig. 3. The expression pattern and protein content, kinase activity of *OsPDK1* and ABA content. (A–D) The expression pattern of *OsPDK1* under ABA (A) and Al (B) treatments, and the protein content (C), kinase activity (D) of OsPDK1 under Al and ABA. Three-day-old rice were treated with or without ABA (A, C, D) for indicated time (0, 15, 30, 45, 60, 90, 120, 180, 240, 360, 720 min), or exposed to 50 μmol L^{-1} $AlCl_3$ at pH 4.5 (B, C, D) for indicated time (0, 3, 6, 12, 24, 36, 60, 84, 96 h), the rice seedlings were collected for gene expression using RT-qPCR, and protein content, kinase activity by immunoprecipitation via anti-OsPDK1. (E) The expression patterns of *OsPDK1* in roots and shoots. Three-day-old rice plants were treated with or without 50 μmol L^{-1} $AlCl_3$ for 12 h at pH 4.5 and the shoots and roots were collected. (F) The root segments (0–5, 5–10 and 10–20 mm) were treatment with 50 μmol L^{-1} $AlCl_3$ at pH 4.5 for 12 h and cut with a razor. Whole roots or shoots were collected (E), root segments were also analyzed (F). (G–H) The expression of *OsPDK1* under different concentration of Al for 12 h and different pH treatments. Tested $AlCl_3$ levels varied from 10 to 100 μmol L^{-1} (0, 10, 25, 50, 100 μmol L^{-1}, at pH 4.5) (G) and a number of pH values were applied (H). (I, J) Al stress induce the accumulation of ABA. The ABA content was detected under 50 μmol L^{-1} $AlCl_3$ at pH 4.5 for different time (0, 0.5, 1, 3, 6, 9, 12, 15 h) (I) and different concentration (0, 10, 25, 50, 100 μmol L^{-1}) of $AlCl_3$ at pH 4.5 for 12 h (J). (K) Expression pattern of *OsPDK1* in the presence of 50 μmol L^{-1} ABA or ABA biosynthesis inhibitor fluridone. Rice seeds were treated with or without fluridone (Flu), an ABA inhibitor, for 8 h, then the plants were treated with 50 μmol L^{-1} ABA for 45/180 min after exposed to 50 μmol L^{-1} $AlCl_3$ at pH 4.5. *OsPDK1* expression level was detected by RT-qPCR, and *Histone3* was an internal control. Datas are means ± SD (n = 3). *, $P < 0.05$.

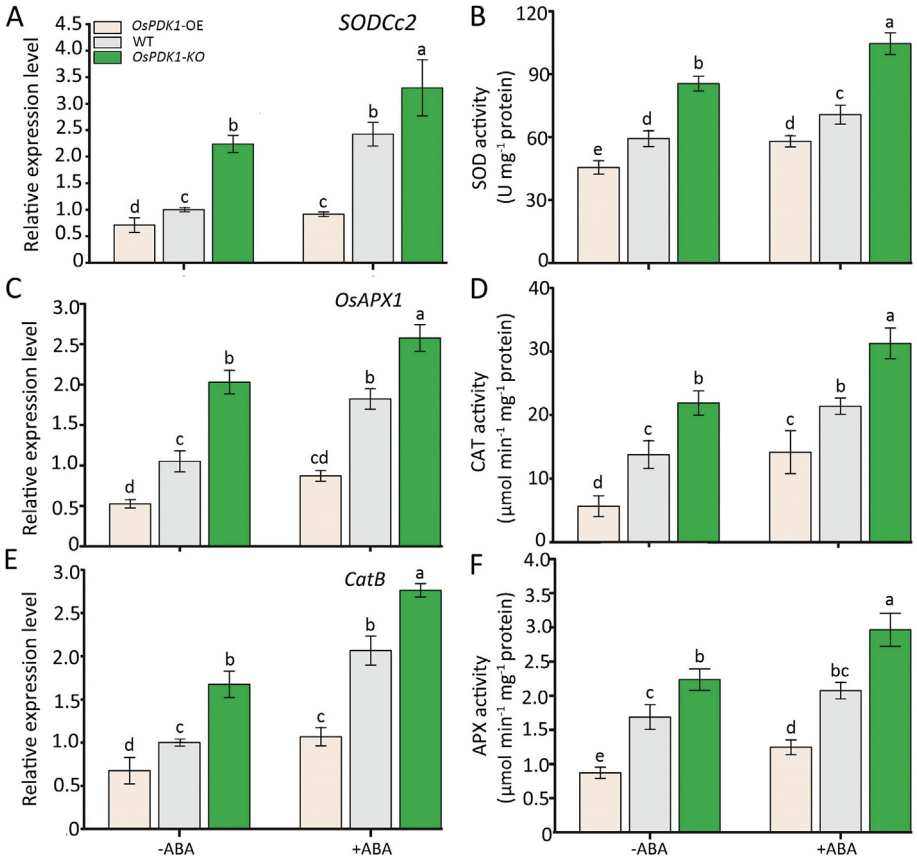

Fig. 4. The expression level of *SODCc2, OsAPX1*, and *OsCatB*, and activities of SOD, CAT, and APX in transgenic rice plants of *OsPDK1*. Rice were treated with or without ABA for 45 min, and expression of *SODCc2, OsAPX1*, and *OsCatB* (A, C, E) and activities of SOD, CAT, and APX (B, D, F) were determined. Data are mean ± SD (n = 3).Means labeled with the same lowercase letter do not differ at $P < 0.05$.

activities of ZFP36 and the promoters of *OsAPX1*, *CatB*, and *SODCc2*. To assess ZFP36′s transcriptional activity, we conducted an *Agrobacterium*-mediated GUS reporter assay with effector and reporter plasmids in tobacco (Fig. 5E–F). ZFP36 increased the promoter activity of *OsAPX1* (Fig. 5E, F), consistent with previous findings [14]. However, the GUS activity in tobacco transfected with the effectors OsPDK1 and ZFP36 showed a significant reduction compared to the effector ZFP36 alone (Fig. 5F). This demonstrates that OsPDK1 can silence *OsAPX1* promoter activity by repressing ZFP36. Huang [3] has previously demonstrated the involvement of OsALS1 in Al tolerance. OsALS1 is also identified as a potential target for ZFP36 via ChIP-Seq [14], and the promoters of *OsALS1* and *OsAPX1* genes contain a conserved C2H2 binding site overlapped in ChIP-seq (Fig. 5I). We conducted an RT-qPCR survey of *OsALS1* expression in *zfp36* mutants (Fig. 5B). ChIP RT-PCR in *ZFP36*-overexpressing plants immunoprecipitated with anti-ZFP36 antibody (Fig. 5D) and yeast one-hybrid assay (Fig. 5C) were employed to corroborate the ChIP-Seq findings. As depicted in Fig. 5B, ZFP36 altered *OsALS1* expression, acting as a positive transcriptional regulator of this gene. ChIP RT-PCR (Fig. 5D) and Y1H (Fig. 5C) demonstrated that ZFP36 directly binds to the upstream segment from (−400 bp) to (+1 bp) (P2) of *OsALS1*.

To further explore the role of OsPDK1 in regulating *OsALS1*, we performed a dual luciferase assay in rice protoplasts. The upstream segment from (−400 bp) to (+1 bp) (P2) of *OsALS1* was inserted in front of the translational initiation site of the renilla luciferase (REN) reporter and served as a putative *cis*-acting element. As indicated in Fig. 5G and H, the LUC/REN ratio was significantly upregulated by ZFP36 and downregulated by OsPDK1. The increase in the LUC/REN ratio caused by ZFP36 decreased in the presence of OsPDK1, suggesting that OsPDK1 suppresses ZFP36 transcriptional activity, thereby impacting the promoter activity of *OsALS1* (Fig. 5G, H).

3.8. OsPDK1 functions upstream of ZFP36 to down-regulate antioxidant enzymes activated by ABA pathway

The interaction between OsPDK1 and ZFP36 inhibits ZFP36-induced ABA-triggered antioxidant defense. Elevated levels of Al^{3+} have been shown to inhibit the expression of *OsPDK1* (Fig. 3B–G) and induce *ZFP36* expression in an ABA-dependent manner (Fig. 1D–F). Both OsPDK1 (Fig. 4) and ZFP36 [13] are essential for ABA-triggered antioxidant defense. Given the confirmed direct interaction between ZFP36 and OsPDK1 (Fig. 2), it is plausible that OsPDK1 influences ABA-induced antioxidant defense to alleviate Al toxicity by interacting with ZFP36. To elucidate the interplay between OsPDK1 and ZFP36 in the regulation of antioxidant systems, we generated rice plants with various genetic modifications: overexpression of both *OsPDK1* and *ZFP36* (*OsPDK1/ZFP36*), overexpression of *OsPDK1* and knock-down of *ZFP36* (*OsPDK1/zfp36*), and knock-out of *OsPDK1* and silencing of *ZFP36* (*ospdk1/zfp36*) through hybridization. The results indicated a reduction in the activities of SOD, CAT, and APX in *OsPDK1/ZFP36* rice plants compared to the *ZFP36* overexpression (*ZFP36*) under ABA treatment (Fig. 6A,–C). In contrast, the activities of SOD, CAT, and APX increased in *OsPDK1*-KO1 rice plants (Fig. 6 A,–C). However, there was no significant increase in the activities of APX, CAT, and SOD in *ospdk1/zfp36* rice plants compared to the control (Fig. 6). ABA-induced elevations of APX, CAT, and SOD activities were inhibited in *ZFP36*-RNAi mutants and *ospdk1/zfp36* mutants

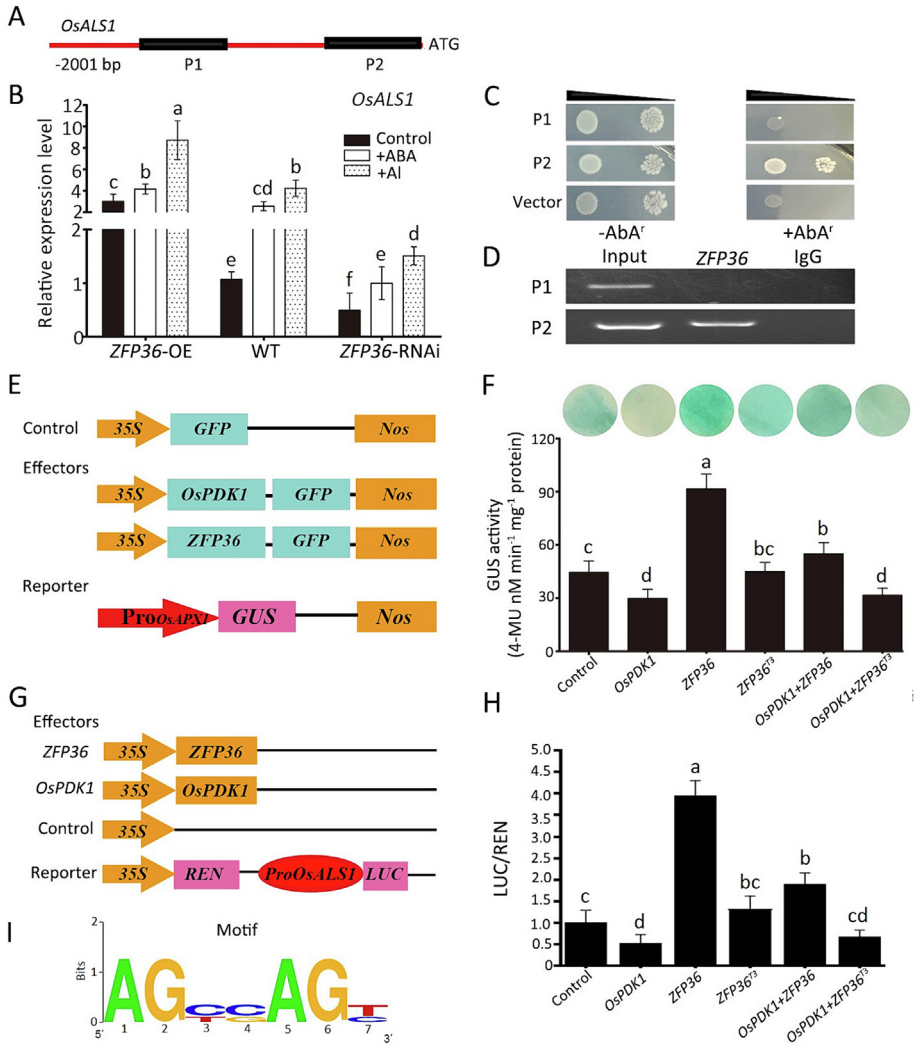

Fig. 5. OsPDK1 inhibits ZFP36 activity via targeting *OsAPX1* or *OsALS1* promoter. (A) Diagram of *OsALS1* promoter locus. P1 ((−1400 bp) to (−900 bp)) and P2 ((−400 bp) to (+1 bp)) stand for two segments of *OsALS1* promoter. (B) ZFP36 changes *OsALS1* expression. Rice plants were treated with 50 μmol L^{-1} ABA for 45 min, and the *OsALS1* expression was determined by RT-qPCR. (C) Yeast one-hybrid assay. The reconstructed pAbAi vector and pGADT7 were co-transformed to yeast strain AH109, the positive clone was confirmed by the growth on the SD/-Leu medium with 300 ng mL^{-1} AbA^r (Aureobasidin A) for 3 d. (D) ChIP assay combined with RT-PCR.Anti-ZFP36 antibody was used to immunoprecipitate fragmented chromatin DNA that may have bound ZFP36. P1 and P2 segments were measured separately by its specific primers. Input stands for the total chromatin DNA before immunoprecipitation, ZFP36 stands for the DNA segments precipitated with anti-ZFP36 antibody, and IgG stands for DNA segments precipitated by mouse IgG. (E) A schematic diagram of the effectors and reporter in tobacco transformation. (F) GUS (β-glucuronidase) activity was used to measure transactivation activity following the co-transformation of effectors and reporter plasmids (shown in (D)) into *N. benthamiana* by *agrobacterium*. (G) A schematic diagram of effectors and reporter in rice protoplast transformation. *35S: ZFP36*/*OsPDK1* fused to pGREENII 62-SK was used as the effector, and the reporter in this experiment was the promoter of OsALS1, which was introduced to pGreenII 0800-LUC, while *35S-* was served as control. (H) The ratio of LUC to Renilla luciferase (REN) contributed to the detection of transactivation activity in rice protoplasts co-transformed with combined effector (s) and reporter shown in (F). Experiments repeated three times showed similar results. $ZFP36^{T3}$ means the full-length of ZFP36 lacking 73–162 aa. Data are mean ± SD (n = 3).Means labeled with the same lowercase letter do not differ at $P < 0.05$. (I) Binding motif investigated in the overlapping ZFP36 binding peaks. The conserved motif is found in the promoters of *OsAPX1* and *OsALS1* genes based on ChIP-seq.

(Fig. 6). *OsPDK1* overexpression and *ZFP36* silencing (*OsPDK1/zfp36*) resulted in a more pronounced decrease in APX, CAT, and SOD activities compared to individual overexpression of *OsPDK1* (*OsPDK1*) or *ZFP36*-RNAi (*zfp36*) (Fig. 6).

4. Discussion

4.1. ABA signaling system contributes to control of Al tolerance in plants

Plants cultivated in acid soils often face challenges associated with heightened activity of Al^{3+}, a prominent ionic form of aluminum. This activity not only impedes root growth but also disrupts cell metabolism [2,35,36]. As plants absorb Al^{3+}, it enters the food chain, posing significant health risks upon accumulation in human bodies. In response to Al^{3+}-induced toxicity, plants have evolved intricate strategies to mitigate damage and reduce Al content [36,37]. These strategies encompass both physiological and genetic adaptive responses, such as the production and excretion of organic ligands to bind Al^{3+} [2,37], relocation of Al^{3+} from the cytoplasm to the apoplastic space and vacuole [3,38], adjustment of metabolic activities [21], reinforcement of free radical defense [39], and activation of "adaptive" genetic programs [40]. One notable strategy involves the ABA-dependent upregulation of antioxidant gene expression [41]. Recent transcriptomic analyses have revealed that treatments involving Al and ABA share approximately one-third of responsive genes, indicating the potential involvement of ABA signaling in the onset of Al tolerance [42]. Previous studies explored the endogenous accumulation of ABA as an

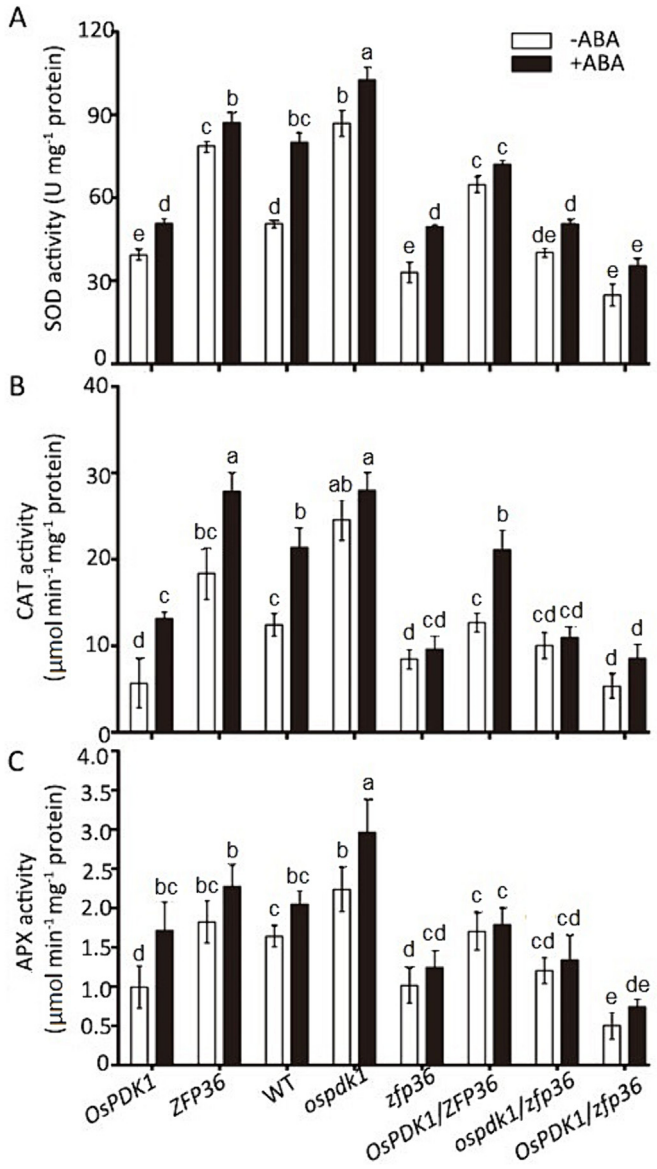

Fig. 6. OsPDK1 acts upstream of ZFP36 in ABA-induced antioxidant defense. (A–C) The activities of SOD (A), CAT (B), and APX (C) in *OsPDK1*-OE1 plants (*OsPDK1*), *ZFP36*-OE plants (*ZFP36*), WT plants (WT), and *OsPDK1*-KO1 plants (*ospdk1*), *ZFP36*-RNAi plants (*zfp36*), and both overexpressing of *OsPDK1* and *ZFP36* plants (*OsPDK1/ZFP36*), knockout of *OsPDK1* and RNA interference of *ZFP36* plants (*ospdk1/ zfp36*), and overexpressing of *OsPDK1* and *RNA* interference *of ZFP36* plants (*OsPDK1/ zfp36*). The plants were treated with (+ABA) or without 50 μmol L^{-1} ABA for 2 h. Bars indicate means ± SD of three independent tests. There is no significant difference between values labeled with the same lowercase letter ($P < 0.05$).

adaptive response to Al stress in soybean [8], buckwheat [43], and barley [44]. While it has been hypothesized that the ABA signaling system contributes an additional layer of regulatory control over Al tolerance in plants [45], the molecular mechanisms underlying this phenomenon remain unclear [46].

4.2. Elucidation of ABA-modulated Al tolerance mediated by OsPDK-ZFP36 complex in rice plants

In this study, employing an integrated approach encompassing physiological, biochemical, and molecular analyses, we elucidate the basis of ABA-modulated Al tolerance in rice plants, focusing on the expression and function of the zinc finger protein ZFP36. Our findings are supported by multiple lines of evidence. Elevated Al^{3+} levels inhibited root elongation and induced ABA accumulation in the roots (Figs. 1A, B, 3I, J). Notably, Al^{3+} and ABA treatments led to the upregulation of *ZFP36* expression (Fig. 1D–F). Plants overexpressing *ZFP36* exhibited improved root elongation under Al treatment compared to wild-type (WT), while plants with reduced *ZFP36* levels (RNAi-mediated *ZFP36* knockdown mutants) displayed heightened sensitivity to Al (Fig. 1). Considering that pH alterations impact the surface charge of the plasma membrane (PM), influencing the concentration of Al on the PM surface, and given the toxicity of protons in acidic solutions, changes in solution pH could potentially modify the speciation of Al [47]. Thus, it is plausible that ZFP36 may influence the solution's pH, thereby affecting Al and proton toxicity for root growth. C2H2 zinc finger proteins, such as ZFP36, interact with other proteins [48,49]. Transcriptional regulation of stress-tolerance genes is a key factor in Al tolerance [21,22]. Through yeast two-hybrid screening, we identified a candidate target for ZFP36, the pyruvate dehydrogenase kinase OsPDK1, which showed *in vivo* and *in vitro* interaction with ZFP36, leading to a reduction in OsPDK1 activity following this interaction (Figs. 2, 5, S4). OsPDK1 displayed initial inhibition followed by activation in response to exogenously applied ABA and Al^{3+} (Fig. 3). Gain- and loss-of-function analyses revealed that high OsPDK1 activity plays a central role in the downregulation of superoxide dismutase (*SODCc2*), catalase (*OsCatB*), ascorbate peroxidase (*OsAPX1*), and the transporter responsible for removing Al^{3+} to the vacuole (*OsALS1*) (Figs. 4, S8). OsPDK1 suppresses ZFP36 transcriptional activity, potentially influencing the expression of *OsAPX1* and *OsALS1* by affecting the promoter activities of *OsAPX1* (Fig. 5E, F) and *OsALS1* (Fig. 5G, H). ABA/ZFP36-induced inhibition of OsPDK1 activity resulted in increased antioxidant capacity and Al sequestration capabilities in rice root cells (Figs. 4, S8). One of the mechanisms for coping with Al toxicity involves the removal of Al^{3+} from the cytosol and its sequestration in the vacuole [2]. This process is catalyzed by two transporters, the tonoplast OsALS1 transporter [3] and the plasma membrane Nrat1 transporter [4,50], with our study revealing the essential role of OsPDK1 in the expression of *Nrat1* (Fig. S8).

4.3. The potential for mis-localization of recombinant proteins should be considered in OsPDK-ZFP36 complex

Our findings introduce a novel dimension to the functional repertoire of OsPDK1 and its interplay with ZFP36. While OsPDK1 has been conventionally recognized for its role as a mitochondrial protein, primarily associated with known pyruvate dehydrogenase (PP) and pyruvate dehydrogenase complex (PDC) functions within the mitochondria [29], our study unveils a previously unexplored aspect. We identify ZFP36 as a newly recognized interacting and regulatory partner for OsPDK1 in the nucleus. In this context, OsPDK1 emerges not only as a participant in mitochondrial processes but also as a regulator of ZFP36, thereby expanding the functional spectrum of OsPDK1. Our findings add to the growing list of proteins regulated by OsPDK1, which already includes OsLEA5 and its homologs [14,15]. While earlier studies highlighted the mitochondrial role of OsPDK1 [29], our investigation reveals its expression in the nucleus as well (Fig. S5). This dual subcellular localization broadens the functional scope of OsPDK1. Concurrently, we observe the expression of *ZFP36* within the nucleus [20], underscoring the significance of their nuclear interactions. This novel aspect of dual localization in both the nucleus and mitochondria advances plant biology. ZFP36 and OsPDK1 function in numerous plant processes, further emphasizing the importance of unraveling their intricate interplay. However, it is crucial to acknowledge the potential for mis-localization of recombinant proteins, and the subcellular location of OsPDK1 should be identified using PDK1-specific antibodies *in situ* in future investigations.

This step will contribute to a more comprehensive and accurate characterization of the subcellular distribution of OsPDK1 and refine our understanding of its versatile cellular roles.

4.4. TCA cycle functions in metabolic pathways that intersect with ABA and ROS signaling in which PDK1 acts

Pyruvic acid, an end product of glycolysis and a crucial substrate for the tricarboxylic acid (TCA) cycle, plays a central role in metabolic pathways that intersect with abscisic acid (ABA) and reactive oxygen species (ROS) signaling [51]. The pyruvate dehydrogenase complex (PDC), composed of three proteins, is instrumental in regulating pyruvate levels, thereby influencing the TCA cycle, cellular energetics, and the biosynthesis of essential macromolecules [30]. PDC activity is intricately controlled through phosphorylation (inhibition) and dephosphorylation (activation), modulated by corresponding kinases (PDKs) and phosphatases (PP) [27,52]. Our study reveals that OsPDK1 acts as a downstream inhibitor of ABA-induced antioxidant defense, with the goal of mitigating aluminum (Al) toxicity. In rice leaves, OsPDK1 expression, protein concentration, and kinase activity exhibit induction following a transient inhibition by ABA and Al (Fig. 4A–D). Notably, we establish a physical interaction between OsPDK1 and ZFP36 proteins, suggesting a potential mechanism for blocking OsPDK1 under Al stress conditions. This interaction could result in the release of antioxidant defense and Al sequestration. ZFP36, previously identified as a regulator by Zhang et al. [13] and Li et al. [20], targets specific genes, including those involved in ABA-induced antioxidant defense, and orchestrates feedback regulation [13,15,20,53]. This implies a complex mechanism underlying Al defense mediated by ZFP36. Consequently, the rice response to Al tolerance via ABA involves intricate interactions that relate to the induction of antioxidant defense and Al-induced redox imbalance [12]. OsPDK1 emerges as a modulator of the ABA/redox-related Al defense in rice, contributing to the intricate regulatory network (Fig. 4).

4.5. ZFP36 plays a different role with other zinc finger proteins coping with Al toxicity

ZFP36 is a member of the extensive zinc finger protein family, and numerous studies across various plant species, including *Arabidopsis*, petunia, soybean, and rice, have indicated their involvement in aluminum (Al) tolerance [16–18,37]. ART1 and ART2 (aluminum resistance transcription factor) in rice and GhSTOP1 in Arabidopsis are key players in Al tolerance, regulating specific Al-resistance genes [54–60]. Phylogenetic analysis reveals that ART1/2 (STOP1) falls in cluster I, characterized by single-fingered proteins with Z2- to Z5-type zinc fingers (ZFs), while ZFP36 belongs to cluster II, featuring proteins with two consecutive Q-type ZFs carrying the conserved sequence "QALGGH" in the DNA-recognition motif [59]. This suggests that different structural types of zinc finger proteins may employ distinct mechanisms in detoxifying Al. *OsALS1*, a target for both ART1 and ZFP36 (Fig. S8), displays redundancy in its regulatory elements, responding to different transcription factors under varying conditions. Co-regulation by a combination of transcription factors is a common phenomenon, exemplified by the presence of "DRE" and "AREB" motifs in promoters of SALT/DROUGHT tolerance genes [60]. *Nramp aluminum transporter* (*Nrat1*) and *OsFRDL4* are induced by ABA (Fig. S7) and are targets for ART1, but not bound by ZFP36 according to ChIP-seq analysis. In contrast, OsPDK1 negatively modulates *OsFRDL4* expression and citrate secretion (Fig. S9), suggesting that OsPDK1 plays an essential role in the rice response to aluminum through distinct pathways. Considering the opposite roles of pyruvate dehydrogenase kinase and pyruvate phosphate dikinase in the citric acid cycle, our findings highlight the intricate interplay in the regulation of organic acid exudation and aluminum accumulation in roots [6]. This work expands our understanding of ZFP36's role in aluminum tolerance, complementing its previously known functions in drought and rice blast tolerance [13,20]. The findings contribute to elucidating a mechanism for plant adaptation to elevated Al^{3+} levels.

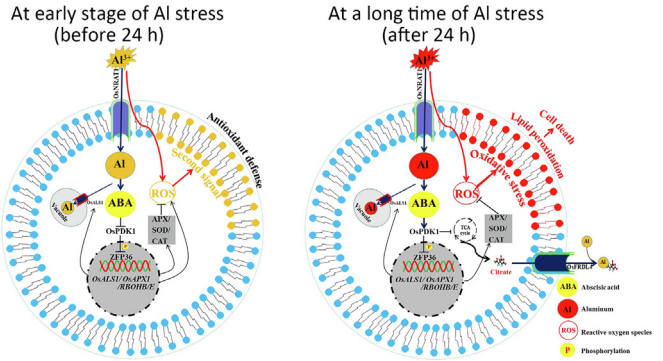

Fig. 7. A hypothetical model describing function of OsPDK1-ZFP36 in ABA-mediated response to Al^{3+} Al stimulates ABA accumulation in roots. At early stage of Al stress (left, before 24 h of Al stress), Al-induced ABA involved the expression of antioxidant defense enzymes (APX, SOD and CAT) to scavenge toxic ROS, ZFP36 could induce the expression of ROS generation via activating the RBOHB/E expression, hence to make the homeostasis of ROS to play the role of second messengers to cope with stresses. Meanwhile, Al-induced ABA could also induce the expression of tonoplast Al transporter *OsALS1* to transport Al^{3+} into vacuole. This process was dependent on activating the transcriptional activity of ZFP36 (through ABA-induced inhibition of OsPDK1 at early stage). At late stage of Al stress (right, after 24 h of Al stress), OsPDK1 was positively activated by ABA with unknown mechanism, the up-expressed OsPDK1 further inhibited the citrate acid exudation possibly via OsFRDL4 transporter, to make TCA cycle homeostasis, and reduce the generation of citrate. ZFP36 was inhibited by OsPDK1, ZFP36 participated in the ABA-mediated antioxidant defense was blocked, ROS was accumulated to result in oxidative stress and lipid peroxidation, thus in the death of plant cells. Taken together, these results elucidate the mechanism of ameliorating Al toxicity via scavenging ROS and promoting Al^{3+} sequestration to the vacuole.

4.6. At late stage of Al stress, OsPDK1 is activated by ABA to maintain TCA cycle homeostasis and alleviate redox imbalance and remove Al^{3+} from the cytosol

We present a schematic model summarizing our hypothesis (refer to the scheme in Fig. 7). Al^{3+} in the rhizosphere penetrates the root cytosol via the OsNRAT1 transporter. In the root cell, some Al^{3+} (either in its free form or as part of an Al-chelate complex) is transported into the vacuole through the OsALS1 transporter. ABA accumulation, facilitated by an as-yet unknown mechanism, induces ROS production by activating up-regulated Rbohs [13], serving as second messengers to initiate antioxidant defense. Our findings indicate that OsPDK1 plays a role in Al tolerance as a negative regulator. *OsPDK1* is induced by ABA following an initial downregulation. It interacts with and inhibits the transcriptional activity of ZFP36. During the early stages of Al stress (Fig. 7, left, before 24 h of Al stress), OsPDK1-mediated inhibition of ZFP36 results in a downregulation of antioxidant enzymes (APX, SOD, and CAT) and reduced Al sequestration in the root cell vacuole through OsALS1. As OsPDK1 inhibition increases, ZFP36 activation becomes more prominent under Al stress conditions. The heightened activity of ZFP36 stimulates ABA-mediated antioxidant defense and Al transporter activity, alleviating redox imbalance and facilitating the removal of Al^{3+} from the cytosol. As Al stress progresses to the late stage (Fig. 7, right, after 24 h of Al stress), OsPDK1 is activated by ABA via an unknown mechanism. The upregulation of *OsPDK1* inhibits the TCA cycle [27] and further

suppresses citric acid exudation, possibly through the OsFRDL4 transporter, to maintain TCA cycle homeostasis and reduce citrate production (Fig. 7). Simultaneously, *ZFP36* is inhibited by OsPDK1, impeding its participation in ABA-mediated antioxidant defense. This leads to the accumulation of ROS, resulting in oxidative stress, lipid peroxidation, and ultimately cell death.

4.7. OsPDK1-ZFP36 modulates ABA-mediated antioxidant defense to scanvenge Al toxicity, and OsPDK1 might possess a potential function in sensing toxic metals

OsPDK1 can interact with and act upstream of *ZFP36* to modulate ABA homeostasis and the activities of antioxidant enzymes in ABA signaling. OsPDK1 exhibits several features commonly associated with proteins involved in heavy metal metabolism, including a heavy metal sensor kinase domain (cztS_silS_copS from 262 aa to 343 aa) (Fig. S3). While aluminum (Al) itself is not formally classified as a heavy metal (molecular weight (MW) = 26.982 g mol^{-1}), it elicits similar defense responses in plant cells [21]. This suggests that OsPDK1 might possess a potential function in sensing toxic metals.

5. Conclusions

A mechanism that enables plants to cope with toxic Al load involves the pyruvate dehydrogenase kinase OsPDK1, which interacts with and phosphorylates ZFP36, contributing to ABA-mediated detoxification of aluminum.

CRediT authorship contribution statement

Nana Su: Conceptualization, Data curation, Funding acquisition, Writing – original draft. **Yanning Gong:** Formal analysis, Validation, Writing – review & editing. **Xin Hou:** Investigation, Methodology. **Xing Liu:** Resources. **Sergey Shabala:** Funding acquisition. **Vadim Demidchik:** Project administration. **Min Yu:** Writing – review & editing. **Mingyi Jiang:** Methodology, Software. **Liping Huang:** Project administration, Supervision, Visualization.

Declaration of competing interest

The authors declare that they have no known competing financial interests or personal relationships that could have appeared to influence the work reported in this paper.

Acknowledgments

We thank Prof. Wenhua Zhang of Nanjing Agricultural University for providing the vectors of pSUPER1300 and pCAMBIA1301. Special thanks to Prof. Hongxuan Lin of Shanghai Institute of Plant Physiology and Ecology, Shanghai Institutes for Biological Sciences, Chinese Academy of Sciences, for supplying the rice protoplast transformation vectors used in investigating TFs transactivation. Financial support for this work was provided by the National Natural Science Foundation of China (31901202, 31672228), National Distinguished Expert Project (WQ20174400441), the Higher Education Department of Guangdong province (2020KCXTD025), Key Laboratory Project of Guangdong Province (2022B1212010015), and the Australian Research Council (DP150101663).

Appendix A. Supplementary data

Supplementary data for this article can be found online at https://doi.org/10.1016/j.cj.2024.06.004.

References

[1] M. Riaz, L. Yan, X.W. Wu, S. Hussain, O. Aziz, Y.H. Wang, M. Imran, C.C. Jiang, Boron alleviates the aluminum toxicity in trifoliate orange by regulating antioxidant defense system and reducing root cell injury, J. Environ. Manage. 208 (2018) 149–158.
[2] J.F. Ma, Syndrome of aluminum toxicity and diversity of aluminum resistance in higher plants, Int. Rev. Cytol. 264 (2007) 225–252.
[3] C.F. Huang, N. Yamaji, Z.C. Chen, J.F. Ma, A tonoplast-localized half-size ABC transporter is required for internal detoxification of aluminum in rice, Plant J. 69 (2012) 857–867.
[4] J.Y. Li, J.P. Liu, D.K. Dong, X.M. Jia, S.R. McCouch, L.V. Kochian, Natural variation underlies alterations in nramp aluminum transporter (NRAT1) expression and function that play a key role in rice aluminum tolerance, Proc. Natl. Acad. Sci. U. S. A. 111 (2014) 6503–6508.
[5] E. Delhaize, P.R. Ryan, P.J. Randall, Aluminum tolerance in wheat (*Triticum aestivum* L.) (II. Aluminum-stimulated excretion of malic acid from root apices), Plant Physiol. 103 (1993) 695–702.
[6] L.I. Trejo-Téllez, R. Stenzel, F.C. Gómez-Merino, J.M. Schmitt, Transgenic tobacco plants overexpressing pyruvate phosphate dikinase increase exudation of organic acids and decrease accumulation of aluminum in the roots, Plant Soil 326 (2010) 187–198.
[7] M.Y. Liu, H.Q. Lou, W.W. Chen, M.A. Piñeros, J.M. Xu, W. Fan, L.V. Kochian, S.J. Zheng, J.L. Yang, Two citrate transporters coordinately regulate citrate secretion from rice bean root tip under aluminum stress, Plant Cell Environ. 41 (2018) 809–822.
[8] H. Shen, A. Ligaba, M. Yamaguchi, H. Osawa, K. Shibata, X.L. Yan, H. Matsumoto, Effect of K-252a and abscisic acid on the efflux of citrate from soybean roots, J. Exp. Bot. 55 (2004) 663–671.
[9] L.J. Wu, Y. Kobayashi, J. Wasaki, H. Koyama, Organic acid excretion from roots: a plant mechanism for enhancing phosphorus acquisition, enhancing aluminum tolerance, and recruiting beneficial rhizobacteria, Soil Sci. Plant Nutr. 64 (2018) 697–704.
[10] W.J. Huang, X.D. Yang, S.C. Yao, T. LwinOo, H.Y. He, A.Q. Wang, C.Z. Li, L.F. He, Reactive oxygen species burst induced by aluminum stress triggers mitochondria-dependent programmed cell death in peanut root tip cells, Plant Physiol. Biochem. 82 (2014) 76–84.
[11] C. Ribeiro, J. Cambraia, P.H.P. Peixoto, E.M.D.F. Júnior, Antioxidant system response induced by aluminum in two rice cultivars, Braz. J. Plant Physiol. 24 (2012) 107–116.
[12] P.M. Kopittke, Role of phytohormones in aluminium rhizotoxicity, Plant Cell Environ. 39 (2016) 2319–2328.
[13] H. Zhang, Y.P. Liu, F. Wen, D.M. Yao, L. Wang, J. Guo, L. Ni, A.Y. Zhang, M.P. Tan, M.Y. Jiang, A novel rice C2H2-type zinc finger protein, ZFP36, is a key player involved in abscisic acid-induced antioxidant defence and oxidative stress tolerance in rice, J. Exp. Bot. 65 (2014) 5795–5809.
[14] L.P. Huang, J. Jia, X.X. Zhao, M.Y. Zhang, X.X. Huang, E. Ji, L. Ni, M.Y. Jiang, The ascorbate peroxidase APX1 is a direct target of a zinc finger transcription factor ZFP36 and a late embryogenesis abundant protein OsLEA5 interacts with ZFP36 to co-regulate OsAPX1 in seed germination in rice, Biochem. Biophys. Res. Commun. 495 (2018) 339–345.
[15] L.P. Huang, M.Y. Zhang, J. Jia, X.X. Zhao, X.X. Huang, E. Ji, L. Ni, M.Y. Jiang, An atypical late embryogenesis abundant protein OsLEA5 plays a positive role in ABA-induced antioxidant defense in *Oryza sativa* L., Plant Cell Physiol. 59 (2018) 916–929.
[16] H. Sakamoto, T. Araki, T. Meshi, M. Iwabuchi, Expression of a subset of the Arabidopsis Cys(2)/His(2)-type zinc-finger protein gene family under water stress, Gene 248 (2000) 23–32.
[17] S. Ciftci-Yilmaz, M.R. Morsy, L.H. Song, A. Coutu, B.A. Krizek, M.W. Lewis, D. Warren, J. Cushman, E.L. Connolly, R. Mittler, The EAR-motif of the Cys2/His2-type zinc finger protein Zat7 plays a key role in the defense response of Arabidopsis to salinity stress, J. Biol. Chem. 282 (2007) 9260–9268.
[18] K. Wang, Y.F. Ding, C. Cai, Z.X. Chen, C. Zhu, The role of C2H2 zinc finger proteins in plant responses to abiotic stresses, Physiol. Plant. 165 (2018) 690–700.
[19] S. Ciftci-Yilmaz, R. Mittler, The zinc finger network of plants, Cell. Mol. Life Sci. 65 (2008) 1150–1160.
[20] W.T. Li, Z.W. Zhu, M. Chern, J.J. Yin, C. Yang, L. Ran, M.P. Cheng, M. He, K. Wang, J. Wang, X.G. Zhou, X.B. Zhu, Z.X. Chen, J.C. Wang, W. Zhao, B.T. Ma, P. Qin, W.L. Chen, Y.P. Wang, J.L. Liu, W.M. Wang, X.J. Wu, P. Li, J.R. Wang, L.H. Zhu, S.G. Li, X.W. Chen, A natural allele of a transcription factor in rice confers broad-spectrum blast resistance, Cell 170 (2017) 114–126.
[21] L.V. Kochian, M.A. Pineros, J.P. Liu, J.V. Magalhaes, Plant adaptation to acid soils: the molecular basis for crop aluminum resistance, Annu. Rev. Plant Biol. 66 (2015) 571–598.
[22] A.A. Daspute, A. Sadhukhan, M. Tokizawa, Y. Kobayashi, S.K. Panda, H. Koyama, Transcriptional regulation of aluminum-tolerance genes in higher plants: clarifying the underlying molecular mechanisms, Front. Plant Sci. 8 (2017) 1358.
[23] M.Y. Jiang, J.H. Zhang, Effect of abscisic acid on active oxygen species, antioxidative defence system and oxidative damage in leaves of maize seedlings, Plant Cell Physiol. 42 (2001) 1265–1273.
[24] J.M. Cao, D.M. Yao, F. Lin, M.Y. Jiang, PEG-mediated transient gene expression and silencing system in maize mesophyll protoplasts: a valuable tool for signal transduction study in maize, Acta Physiol. Plant. 36 (2014) 1271–1281.

[25] L. Ni, X.P. Fu, H. Zhang, X. Li, X. Cai, P.P. Zhang, L. Liu, Q.W. Wang, M.M. Sun, Q. W. Wang, A.Y. Zhang, Z.G. Zhang, M.Y. Jiang, Abscisic acid inhibits rice protein phosphatase PP45 via H_2O_2 and relieves repression of the Ca^{2+}/CaM-dependent protein kinase DMI3, Plant Cell 31 (2019) 128–152.
[26] T.R. Hurd, Y. Collins, I. Abakumova, E.T. Chouchani, B. Baranowski, I.M. Fearnley, T.A. Prime, M.P. Murphy, A.M. James, Inactivation of pyruvate dehydrogenase kinase 2 by mitochondrial reactive oxygen species, J. Biol. Chem. 287 (2012) 35153–35160.
[27] A. Tovar-Mendez, J.A. Miernyk, D.D. Randall, Regulation of pyruvate dehydrogenase complex activity in plant cells, Eur. J. Biochem. 270 (2003) 1043–1049.
[28] J.J. Thelen, M.G. Muszynski, J.A. Miernyk, D.D. Randall, Molecular analysis of two pyruvate dehydrogenase kinases from maize, J. Biol. Chem. 273 (1998) 26618–26623.
[29] A. Jan, H. Nakamura, H. Handa, H. Ichikawa, H. Matsumoto, S. Komatsu, Gibberellin regulates mitochondrial pyruvate dehydrogenase activity in rice, Plant Cell Physiol. 47 (2006) 244–253.
[30] J.J. Thelen, J.A. Miernyk, D.D. Randall, Pyruvate dehydrogenase kinase from *Arabidopsis thaliana*: a protein histidine kinase that phosphorylates serine residues, Biochem. J. 349 (2000) 195–201.
[31] R.J. Li, Z.Y. Hu, H.S. Zhang, G.M. Zhan, H.Z. Wang, W. Hua, Cloning and functions analysis of a pyruvate dehydrogenase kinase in Brassica napus, Plant Cell Rep. 30 (2011) 1533–1540.
[32] M. Houde, A.O. Diallo, Identification of genes and pathways associated with aluminum stress and tolerance using transcriptome profiling of wheat near-isogenic lines, BMC Genomics 9 (2008).
[33] Y. Zhu, J.W. Yan, W.J. Liu, L. Liu, Y. Sheng, Y. Sun, Y.Y. Li, H.V. Scheller, M.Y. Jiang, X.L. Hou, L. Ni, A.Y. Zhang, Phosphorylation of a NAC transcription factor by a calcium/calmodulin-dependent protein kinase regulates abscisic acid-induced antioxidant defense in maize, Plant Physiol. 171 (2016) 1651–1664.
[34] F.F. Ma, L. Ni, L.B. Liu, X. Li, H. Zhang, A.Y. Zhang, M.P. Tan, M.Y. Jiang, ZmABA2, an interacting protein of ZmMPK5, is involved in abscisic acid biosynthesis and functions, Plant Biotechnol. J. 14 (2016) 771–782.
[35] Y.S. Wu, Z.L. Yang, J.Y. How, H.N. Xu, L.M. Chen, K.Z. Li, Overexpression of a peroxidase gene (AtPrx64) of Arabidopsis thaliana in tobacco improves plant's tolerance to aluminum stress, Plant Mol. Biol. 95 (2017) 157–168.
[36] X.W. Li, Y.L. Li, J.W. Mai, L. Tao, M. Qu, J.Y. Liu, R.F. Shen, G.L. Xu, Y.M. Feng, H.D. Xiao, L.S. Wu, L. Shi, S.X. Guo, J. Liang, Y.Y. Zhu, Y.M. He, F. Baluska, S. Shabala, M. Yu, Boron alleviates aluminum toxicity by promoting root alkalization in transition zone via polar auxin transport, Plant Physiol. 177 (2018) 1254–1266.
[37] Y. Zhang, J. Zhang, J.L. Guo, F.L. Zhou, S. Singh, X. Xu, Q. Xie, Z.B. Yang, C.F. Huang, F-box protein RAE1 regulates the stability of the aluminum-resistance transcription factor STOP1 in Arabidopsis, Proc. Natl. Acad. Sci. U. S. A. 116 (2018) 319–327.
[38] J.F. Ma, Z.C. Chen, R.F. Shen, Molecular mechanisms of Al tolerance in gramineous plants, Plant Soil 381 (2014) 1–12.
[39] P.R. Ryan, E. Delhaize, D.L. Jones, Function and mechanism of organic anion exudation from plant roots, Annu. Rev. Plant Physiol. Plant Mol. Biol. 52 (2001) 527–560.
[40] J.F. Ma, P.R. Ryan, E. Delhaize, Aluminium tolerance in plants and the complexing role of organic acids, Trends Plant Sci. 6 (2001) 273–278.
[41] A. Ranjan, R. Sinha, S.K. Lal, S.K. Bishi, A.K. Singh, Phytohormone signalling and cross-talk to alleviate aluminium toxicity in plants, Plant Cell Rep. 40 (2021) 1331–1343.
[42] W. Fan, J.M. Xu, P. Wu, Z.X. Yang, H.Q. Lou, W.W. Chen, J.F. Jin, S.J. Zheng, J.L. Yang, Alleviation by abscisic acid of Al toxicity in rice bean is not associated with citrate efflux but depends on ABI5-mediated signal transduction pathways, J. Integr. Plant Biol. 61 (2019) 140–154.
[43] I. Reyna-Llorens, I. Corrales, C. Poschenrieder, J. Barcelo, R. Cruz-Ortega, Both aluminum and ABA induce the expression of an ABC-like transporter gene (FeALS3) in the Al-tolerant species *Fagopyrum esculentum*, Environ. Exp. Bot. 111 (2015) 74–82.
[44] M. Kasai, M. Sasaki, S. Tanakamaru, Y. Yamamoto, H. Matsumoto, Possible involvement of abscisic acid in increases in activities of two vacuolar H^+ -pumps in barley roots under aluminum stress, Plant Cell Physiol. 34 (1993) 1335–1338.
[45] N.N. Hou, J.F. You, J.D. Pang, M.Y. Xu, G. Chen, Z.M. Yang, The accumulation and transport of abscisic acid in soybean (*Glycine max* L.) under aluminum stress, Plant Soil 330 (2010) 127–137.
[46] Y. Kim, M.D. Kim, S. Park, J.C. Jeong, S. Kwak, H. Lee, Transgenic potato plants expressing the cold-inducible transcription factor SCOF-1 display enhanced tolerance to freezing stress, Plant Breed. 135 (2016) 513–518.
[47] Y. Kobayashi, Y. Kobayashi, T. Watanabe, J.E. Shaff, H. Ohta, L.V. Kochian, T. Wagatsuma, T.B. Kinraide, H. Koyama, Molecular and physiological analysis of Al^{3+} and H^+ rhizotoxicities at moderately acidic conditions, Plant Physiol. 163 (2013) 180–192.
[48] K.J. Brayer, D.J. Segal, Keep your fingers off my DNA: Protein-protein interactions mediated by C2H2 zinc finger domains, Cell Biochem. Biophys. 50 (2008) 111–131.
[49] G.L. Han, C.X. Lu, J.R. Guo, Z.Q. Qiao, N. Sui, N.W. Qiu, B.S. Wang, C2H2 zinc finger proteins: master regulators of abiotic stress responses in plants, Front. Plant Sci. 11 (2020) 115.
[50] J. Xia, N. Yamaji, T. Kasai, J.F. Ma, Plasma membrane-localized transporter for aluminum in rice, Proc. Natl. Acad. Sci. U. S. A. 107 (2010) 18381–18385.
[51] J.L. Shen, C.L. Li, M. Wang, L.L. He, M.Y. Lin, D.H. Chen, W. Zhang, Mitochondrial pyruvate carrier 1 mediates abscisic acid-regulated stomatal closure and the drought response by affecting cellular pyruvate content in *Arabidopsis thaliana*, BMC Plant Biol. 17 (2017).
[52] B.J. Budde, T.K. Fang, D.D. Randall, Regulation of the phosphorylation of mitochondrial pyruvate dehydrogenase complex in situ: effects of respiratory substrates and calcium, Plant Physiol. 88 (1988) 1031–1036.
[53] F. Wen, T.T. Qin, Y. Wang, W. Dong, A.Y. Zhang, M.P. Tan, M.Y. Jiang, OsHK3 is a crucial regulator of abscisic acid signaling involved in antioxidant defense in rice, J. Integr. Plant Biol. 57 (2015) 213–228.
[54] T. Tsutsui, N. Yamaji, J.F. Ma, Identification of a cis-acting element of ART1, a C2H2-type zinc-finger transcription factor for aluminum tolerance in rice, Plant Physiol. 156 (2011) 925–931.
[55] J. Che, T. Tsutsui, K. Yokosho, N. Yamaji, J.F. Ma, Functional characterization of an aluminum (Al)-inducible transcription factor, ART2, revealed a different pathway for Al tolerance in rice, New Phytol. 220 (2018) 209–218.
[56] S. Iuchi, H. Koyama, A. Iuchi, Y. Kobayashi, S. Kitabayashi, Y. Kobayashi, T. Ikka, T. Hirayama, K. Shinozaki, M. Kobayashi, Zinc finger protein STOP1 is critical for proton tolerance in Arabidopsis and coregulates a key gene in aluminum tolerance, Proc. Natl. Acad. Sci. U. S. A. 104 (2007) 9900–9905.
[57] Y. Sawaki, S. Iuchi, Y. Kobayashi, Y. Kobayashi, T. Ikka, N. Sakurai, M. Fujita, K. Shinozaki, D. Shibata, M. Kobayashi, H. Koyama, STOP1 regulates multiple genes that protect arabidopsis from proton and aluminum toxicities, Plant Physiol. 150 (2009) 281–294.
[58] A. Kundu, S. Das, S. Basu, Y. Kobayashi, Y. Kobayashi, H. Koyama, M. Ganesan, GhSTOP1, a C2H2 type zinc finger transcription factor is essential for aluminum and proton stress tolerance and lateral root initiation in cotton, Plant Biol. 21 (2018) 35–44.
[59] P. Agarwal, R. Arora, S. Ray, A.K. Singh, V.P. Singh, H. Takatsuji, S. Kapoor, A.K. Tyagi, Genome-wide identification of C2H2 zinc-finger gene family in rice and their phylogeny and expression analysis, Plant Mol. Biol. 65 (2007) 467–485.
[60] K. Maruyama, D. Todaka, J. Mizoi, T. Yoshida, S. Kidokoro, S. Matsukura, H. Takasaki, T. Sakurai, Y.Y. Yamamoto, K. Yoshiwara, M. Kojima, H. Sakakibara, K. Shinozaki, K. Yamaguchi-Shinozaki, Identification ofcis-acting promoter elements in cold- and dehydration-induced transcriptional pathways in Arabidopsis, rice, and soybean, DNA Res. 19 (2012) 37–49.